PHYSICAL REVIEW B

CONDENSED MATTER

THIRD SERIES, VOLUME 30, NUMBER 2 15 JULY 1984

Photoemission spectra and band structures of d-band metals. XI. Inverse photoemission from Pd(111)

D. A. Wesner and P. D. Johnson
Brookhaven National Laboratory, Upton, New York 11973

N. V. Smith
AT&T Bell Laboratories, Murray Hill, New Jersey 07974

(Received 22 February 1984)

Momentum-resolved inverse photoemission spectra have been taken on Pd(111) at $\hbar\omega = 9.7$ eV. In addition to the unoccupied part of the d band, we observe an s,p peak which disperses, but lies somewhat higher in energy (by ~ 0.5 eV) than a bulk direct-transition peak predicted by band-structure calculations. The s,p peak does not fall in the fundamental s,p gap, and is therefore not attributable to a surface state. A step structure close to the vacuum level is attributed to band-gap emission and image-potential states.

I. INTRODUCTION

It has recently been demonstrated that $\vec{k}$-resolved inverse photoemission (KRIPES) can be used to map the unoccupied energy bands of solids.[1-3] In this paper we report KRIPES measurements on Pd(111) and, in continuation of the unifying theme of this series of papers, we relate the results to the bulk band structure using a combined interpolation scheme.[4,5] Contrary to conclusions published previously by two of the present authors,[6] we no longer find a spectral peak in the fundamental gap of Pd(111), and so the surface-state interpretation of that paper is retracted. We show that an interpretation based on direct transitions within the bulk band structure is in reasonable accord with the data, but some discrepancies in energy (~ 0.5 eV) still remain. We discuss evidence for surface resonances and image-potential states.

II. EXPERIMENTAL MEASUREMENTS

A. Method

The experiments were performed using a band-pass Geiger-Müller detector $\hbar\omega = (9.7 \pm 0.35)$ eV, a commercial electron gun, and a set of retarding grids as described elsewhere.[3] These components, however, were transferred to a different vacuum chamber, made of μ-metal and having low-energy electron diffraction (LEED) and Auger spectroscopy for sample characterization. The distance between the sample and entrance aperture of the detector was increased making the total range of angles of photon collection smaller ($\Delta\theta_{\rm ph} \sim 10°$) than in Ref. 3. For normal incidence of the electrons $\theta_e = 0°$, the mean angle of photon collection is $\bar{\theta}_{\rm ph} = 45°$. The angle of electron incidence is varied by rotating the sample, thus varying $\bar{\theta}_{\rm ph}$ by the same amount. Data was taken on both sides of normal, $\theta_e = 0°$, to test for misalignments or spurious deflections of the electron beam.

The Fermi level E_F in the spectra was located using established procedures, and is consistent (± 0.1 eV) with that found for Cu(001) using the same apparatus.[1] The experimental location of E_F will be of importance when we come to consider the bulk-band-structure dispersion and the evidence for image-potential surface states.

The sample surface was prepared by the usual cycles of ion bombardment and annealing. Auger analysis indicated that the major contaminant, sulfur, was present only to the extent of $< 2\%$ of a monolayer.

B. Results

Figure 1 shows some typical KRIPES data on Pd(111) taken as a function of electron-incidence angle θ_e in the $\bar{\Gamma}\bar{K}$ azimuth. For normal incidence, a prominent peak is seen just above the Fermi level E_F. On increasing θ_e this peak splits into two peaks, one of which remains close to E_F and one which disperses to higher energies.

These results are qualitatively similar to those reported earlier,[6] but there are significant quantitative differences. The results of Ref. 6 can be understood by assuming that there was a misalignment of θ_e by 5°—10° in those experiments.

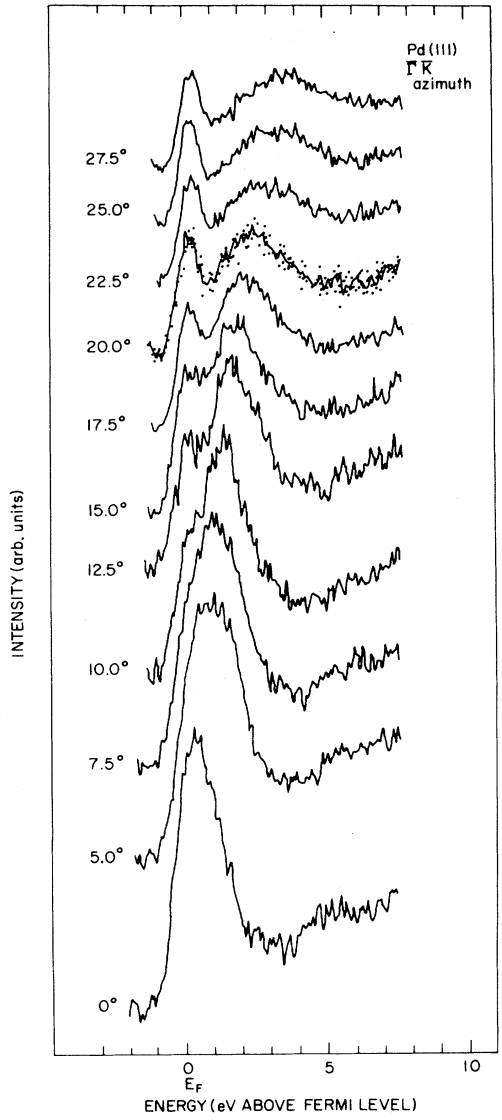

FIG. 1. Inverse photoemission spectra from Pd(111) as a function of angle of electron incidence θ_e. Original data points are shown for $\theta_e = 20.0°$; the other spectra are smoothed.

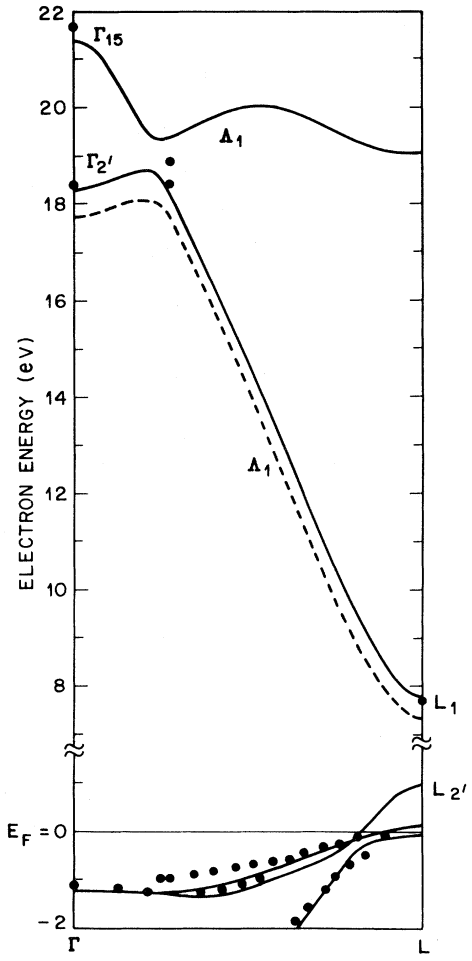

FIG. 2. Empirical band structure of Pd (solid curves) along ΓL is compared with the angle-resolved photoemission data of Ref. 9 (solid circles). The dashed curve is Λ_1 band of the first-principles calculation of Christensen (Ref. 7).

III. BAND-STRUCTURE INTERPRETATION

A. Empirical band structure

Here we use the combined interpolation scheme described earlier.[5] The parameters of the scheme were first fitted to the first-principles relativistic band calculation by Christensen.[7,8] Small adjustments were then made to the parameters in order to reproduce the unoccupied energy levels determined in the angle-resolved photoemission experiments of Himpsel and Eastman.[9] A comparison for the ΓL direction, appropriate to normal emission from Pd(111), is shown in Fig. 2. The first-principles free-electron-like Λ_1 band of Ref. 7 (shown in Fig. 2 as the dashed curve) has been shifted up in energy by 0.5—0.7 eV in the present parametrization. Having arrived at a parametrized band structure, we then generate a theoretical $E_f(k_{||})$ dispersion curve for direct transitions from initial band $i = 7$ into final band $f = 6$.

B. Comparison with experiment

The theoretical $E_f(k_{||})$ dispersion relation (solid curve) is compared in Fig. 3 with the experimental peak positions. Also shown (dashed curve) is the prediction of a simpler nearly-free-electron (NFE) model obtained by fitting the s,p band gap at L.

The strongly dispersing peak seen in experiment falls as much as 2 eV higher than the NFE prediction. The discrepancy is much reduced for the combined-interpolation-scheme prediction. Part of this improvement (≈ 0.2 eV) is due to the adjustments made to reproduce the angle-resolved photoemission data. The largest part of the improvement, however, is a consequence of the hybridization with the Pd d bands which is explicitly included in the combined interpolation scheme but is absent in the NFE model. The main effect of the hybridization

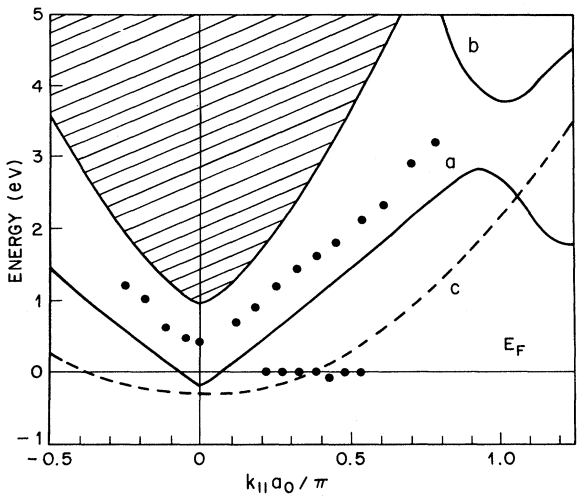

FIG. 3. Comparison between theory and experiment for the $E_f(k_{||})$ relation. Solid circles: experimental data. Solid curves *a* and *b*: direct-transition prediction using the combined-interpolation scheme. Dashed curve *c*: NFE model. The crosshatched area corresponds to the fundamental band gap.

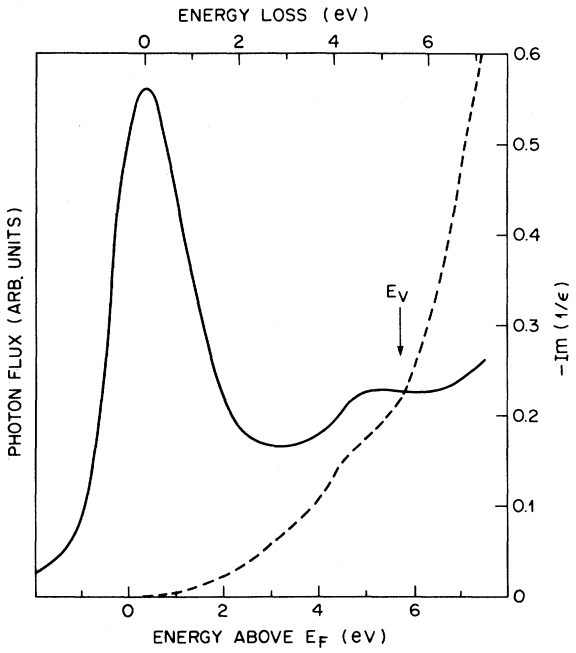

FIG. 4. Normal-incidence KRIPES spectrum on Pd(111) (solid curve) showing the image-potential-state feature near the vacuum level E_V. The dashed curve is the energy-loss function $|\mathrm{Im}(1/\epsilon)|$.

is a mutual repulsion between the respective energy levels, forcing the unoccupied *s,p* levels to higher energy. The use of the combined interpolation scheme, or some other way of including *d* hybridization, is then essential to an understanding of the $E_f(k_{||})$ dispersion of the *s,p* peak.

The lower-energy peak seen experimentally is dispersionless and is positioned very close to E_F. This is attributed to transitions into the unoccupied part of the Pd *d* band. Direct transitions into the *d* band are not permitted at $\hbar\omega = 9.7$ eV, and so we identify this peak as a "density-of-states" feature associated with evanescent wave functions and the concomitant relaxation of strict $k_\perp$ conservation.

IV. SURFACE-STATE DISCUSSION

A. Surface-resonance possibility

While the experimental energy positions for the *s,p* peak still lie higher than our best bulk-band-structure prediction, they do *not*, as previously claimed,[6] fall in the fundamental gap (shown crosshatched in Fig. 3). The simple surface-state interpretation of Ref. 6 is therefore withdrawn.

Self-consistent pseudopotential calculations by Louie[10] predict a surface state very close to the bottom of the gap, which persists as a surface resonance upon increasing $k_{||}$. The experimentally observed *s,p* peak could conceivably be a composite of the expected surface resonance and the bulk direct transition already described. Such an interpretation would serve to explain the remaining discrepancy in energy, but should be regarded as very tentative since the discrepancies are comparable with the uncertainties associated with energy resolution, momentum resolution, and angular alignment. Future experiments with better resolution and tunability of $\hbar\omega$ should remove the present near degeneracy.

B. Image-potential states and band-gap emission

The spectra near normal incidence show a steplike structure just below the vacuum level E_V and this structure shows some discernible dispersion. A similar feature has been seen in Cu(001) and Ni(001),[3] and it has been interpreted by Johnson and Smith in terms of the surface states associated with the long-range nature of the image potential.[11] These authors however were not able to eliminate an alternative interpretation involving energy-loss satellites.

The normal-incidence spectrum is compared in Fig. 4 with the energy-loss function $-\mathrm{Im}(1/\epsilon)$ taken from the optical-data compilation of Weaver *et al.*[12] The absence of any strong structure in $-\mathrm{Im}(1/\epsilon)$ at the appropriate energy permits us to eliminate the energy-loss—satellite interpretation and to concentrate our discussion on the image-potential states.

The emission mechanism giving rise to the step can be viewed as the analog of "band-gap emission" which is well established in ordinary photoemission. In a range of E and $k_{||}$ where bulk states are forbidden, the wave functions are envisaged as LEED wave functions, that is, of propagating form in vacuum and evanescent form within the bulk. Some wave functions are depicted schematically in Fig. 5. Inverse band-gap emission occurs when an incoming electron such as (a) decays radiatively into a band-gap state such as (b). This mechanism should give a contribution to the spectrum which is continuous, but with a low-energy cutoff at E_V. At energies below E_V, the mechanism will give rise to discrete contributions corresponding to the bound surface states within the gap.

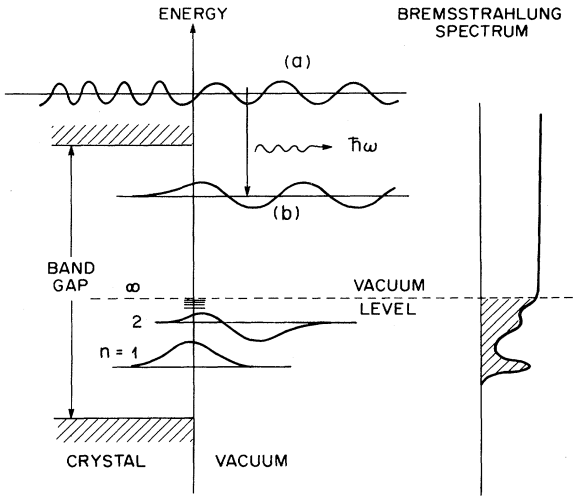

FIG. 5. Electron wave functions near the surface of a metal having a bulk band gap. On the right is a schematic representation of the contributions to the inverse photoemission spectrum due to band-gap—emission processes, with crosshatching used to emphasize those contributions involving bound surface states or resonances.

We need to consider both conventional surface states and image-potential states.

Image-potential states have been considered by a number of authors and reviewed by McRae.[13] In one approach the energy levels of the image-potential state are given by

$$E(k_{||})=E_V-e_n+\hbar^2k_{||}^2/2m \ , \qquad (1)$$

with the binding energy (in Ry) given by the series

$$e_n=1/[16(n+a)^2] \ , \quad n=1,2,\ldots \qquad (2)$$

where the quantum defect parameter a can range between $-\frac{1}{2}$ and $+\frac{1}{2}$ depending on the phase relations for electron scattering in the surface region. The respective values for e_1 range between 3.4 and 0.4 eV. It is tempting (though not obviously essential) to identify the $n=1$ level with the band-gap surface state predicted in conventional short-range theories. At $\bar{\Gamma}$ in Pd(111), Louie[10] places this level a few tenths of an electron volt above the bottom of the band gap. This would imply $e_1 \approx 4.5$ eV, a value outside the range permitted by Eq. (2). This is not a problem since the $n=1$ wave function probes the outermost atomic layer, and the rather restrictive conditions under which Eqs. (1) and (2) are derived need not apply. We have suggested above that this state may be buried under the bulk direct-transition peak discussed in Sec. III.

In this approach, the spectral structure below E_V is interpreted as the unresolved composite of the $n=2$ and higher components of the Rydberg series. Note that a step is to be expected from the termination of the continuum of unbound band-gap states which are propogating in the vacuum. The existence of the image-potential bound states is inferred from the observation that the edge of the step occurs *below* E_V by a distance (≈ 1.3 eV) that cannot be accounted for by finite-resolution smearing (± 0.35 eV). Experiments at higher resolution and at different photon energies would clearly be desirable in order to settle the question concerning the identification of the $n=1$ level and to separate some of the individual components of the Rydberg series.

[1]D. P. Woodruff and N. V. Smith, Phys. Rev. Lett. **48**, 283 (1982).
[2]G. Denninger, V. Dose, M. Glöbl, and H. Scheidt, Solid State Commun. **42**, 583 (1982).
[3]D. P. Woodruff, N. V. Smith, P. D. Johnson, and W. A. Royer, Phys. Rev. B **26**, 2943 (1982).
[4]N. V. Smith and L. F. Mattheiss, Phys. Rev. B **9**, 1341 (1974).
[5]N. V. Smith, Phys. Rev. B **19**, 5019 (1979).
[6]P. D. Johnson and N. V. Smith, Phys. Rev. Lett. **49**, 290 (1982).
[7]N. E. Christensen, Phys. Rev. B **14**, 3446 (1976).
[8]R. Lässer and N. V. Smith, Phys. Rev. B **25**, 806 (1982).
[9]F. J. Himpsel and D. E. Eastman, Phys. Rev. B **18**, 5236 (1978).
[10]S. G. Louie, Phys. Rev. Lett. **40**, 1525 (1978).
[11]P. D. Johnson and N. V. Smith, Phys. Rev. B **27**, 2527 (1983).
[12]J. H. Weaver, C. Krafka, D. W. Lynch, and E. E. Koch, in *Optical Properties of Metals* (Physics Data, Fachinformationszentrum, Karlsruhe, 1981).
[13]E. G. McRae, Rev. Mod. Phys. **51**, 541 (1971).